UW Journal of Science and Technology Vol. 6 (2022) 9-18
ISSN: 2523-0123 (Print) 2616-4396 (Online)

University of Wah
Journal of Science and Technology

www.uow.edu.pk

Study of Flexural Behavior of High Strength Concrete Beams Reinforced with GFRP Bars

Jahanzaib, Huzaifah Hameed, Shahbaz Ahmad, Rashid Hameed and Syed Asad Ali Gillani

***Abstract*—This paper presents the test results of an experimental program which consisted of 8 beams with 100 x 200 mm cross-sectional dimensions. The beams were tested under four-point loading with an effective span length of 1665mm. Of the eight beams, four beams were reinforced with GFRP bars and the remaining four beams were reinforced with steel bars. The load-deflection behavior of the high-strength concrete beams reinforced with GFRP bars showed a bi-linear response, while the beams reinforced with steel bars displayed a tri-linear response. The increase in the longitudinal reinforcement ratio and concrete strength resulted in the improvement of flexural capacity, stiffness and ductility of the beams. Frequent drops in the loading were observed in GFRP RC beams while no drops were observed in the case of steel-reinforced beams. This can be attributed to the weak bond of GFRP bars to concrete. Additionally, the layered sectional analysis program, Response-2000, was used to simulate the behavior of the beams, and the ratios of predicted to experimental peak load values were found to be varying from 0.90 to 0.95.**

***Index Terms*—GFRP bars, concrete, Beams, Flexural response, Concrete strength, Reinforcement ratio, Bi-linear, Tri-linear, Sectional analysis**

I. INTRODUCTION

RECENTLY, the most used construction material is concrete and the broadly used reinforcement technique is the steel reinforcement. The reinforced concrete has been plagued by steel corrosion problems, especially for the structures subjected to a corrosive environment [1].

Manuscript received: Sep 22, 2021; accepted: Oct 4, 2022.

Jahanzaib (email:jahanzaib@mail.utoronto.ca) is affiliated with Civil and Mineral Engineering Department, University of Toronto, ON, M5S 1A4, Canada.

H. Hameed (email:huzaifah.huzi@gmail.com) R. Hameed (email:rashidmughal@uet.edu.pk) and S.A.A. Gillani (email:asadgillani@uet.edu.pk) are affiliated with Civil Engineering Department, University of Engineering and Technology, Lahore, Punjab, Pakistan.

S. Ahmad (email:shahbaz.klasra@gmail.com) is affiliated with Communication and Works Department, Government of Punjab, Pakistan.

*Corresponding author: email:jahanzaib@mail.utoronto.ca

Significant research has been carried out to improve the protection of steel reinforcement by increasing concrete cover, impenetrability, etc. however, the economic impact of steel corrosion has been increased considerably. Over the past few decades, researchers have tried epoxy-coated steel bars and stainless-steel bars to avoid the corrosion issue in the reinforced concrete [2] and implemented air entrainment in concrete. Again, stainless steel reinforcement is proving too costly. Therefore, researchers started studying the alternative reinforcement approaches rather than the steel [2-4]. The use of alternatives to ordinary reinforcing steel is much more adapted nowadays in most countries.

Fiber-reinforced polymer (FRP) bar is a viable alternative available to ordinary steel bars in RC infrastructure [5]. FRP is made up of two main constituents: resin and fibers. Fibers are used to carry the load, and the resin creates the bond between the fibers. Three different types of fibers are generally used in manufacturing the FRP bars and those fibers are glass, carbon and aramid. To repair the existing structurally damaged elements, FRP sheets are used as external reinforcement for beams [6,9] and slabs [7,10] to strengthen. Mostly, FRP sheets are used to repair the columns in bridges [8]. External reinforcement provides additional confinement and strength to weakened structures. The usage of FRP bars among the civil engineering community is expanding with time. This is because of its enormous characteristics compared to conventional reinforcement (steel re-bars). Due to its non-corrosive behavior, such a type of reinforcement is especially practical for marine infrastructure including piers and bridge decks. Moreover, this is particularly valuable in reducing maintenance costs required for repairing. This field is important because civil or marine infrastructure reinforced with steel could be subjected to corrosion in an aggressive environment. In addition, FRP bars are also advantageous in enhancing the loading carrying capacity of RC beams cast using high-strength concrete [11]. Further, increasing the FRP longitudinal reinforcement ratio is a major factor in improving the load-carrying capacity and controlling deflections [12].

Thus, to address the issue of steel corrosion, the flexural response of simply supported beams reinforced with the GFRP re-bars was explored in this study. The study comprised two key phases: study the response of steel reinforced and GFRP reinforced concrete beams. The current study demonstrated several findings concerning the flexural response of GFRP and steel-reinforced concrete beams. GFRP re-bars are made of composite fibers and possess several excellent properties: better fatigue life, high strength to weight ratio, high tensile rupture strength and non-conductivity property. When implementing the FRP bars in RC members, the structural performance of the members is influenced by many properties: higher tension strength, lower elastic module; and bond behavior. [13-16]. For the same reinforcement ratio, beams reinforced with GFRP bars showed higher deflections and larger crack widths than the beams reinforced with steel bars [17]. This can be attributed to the low elastic modulus (35 to 51 GPa) of GFRP bars [18]. Furthermore, the stress-strain behavior of FRP bars is linear until the rupture point and shows no yielding [19].

II. MATERIALS AND METHODS

Eight beams were subjected to the third point bending test in this study. Four beams were reinforced with the Steel bars (two with 2 - # 10 and two with 2 - # 13) and the remaining four with the GFRP bars (two with 2 - # 10 and two with 2 - # 13). The tests were carried out to check the behavior of the beams under the flexural loading. The concrete used was high-strength concrete with a minimum compressive strength of 6000 psi or 42 MPa at 28 days. After the testing, program Response-2000 was used to predict the capacities of the GFRP beams, as well as mid-span deflection. The predicted values of capacity and deflection were compared with experimental data.

A. Test Program

As mentioned earlier, a total of 8 beams were cast with cross-sectional dimensions of 100mm ×200 mm and an effective span of 1665 mm between the supports. The experimental testing stage was divided into two series. The first group consisted of four beams reinforced with GFRP bars, and the second group included the remaining four beams reinforced with steel bars. Testing was conducted under the four-point loading. The parameters examined were the load-deflection responses, cracking behavior and the modes of failure. Each of the series was further divided into the two groups with main variables as the reinforcement ratio (ρ_f) and compressive strengths (f'c). In each series, two beams were cast with 2-#10 bars and the other two with the 2-#13 bars providing the reinforcement ratios of 0.835% and 1.53%, respectively. These different groups are explained in *Fig. 1*.

The breakdown of specimens has been illustrated in *Fig.2*.

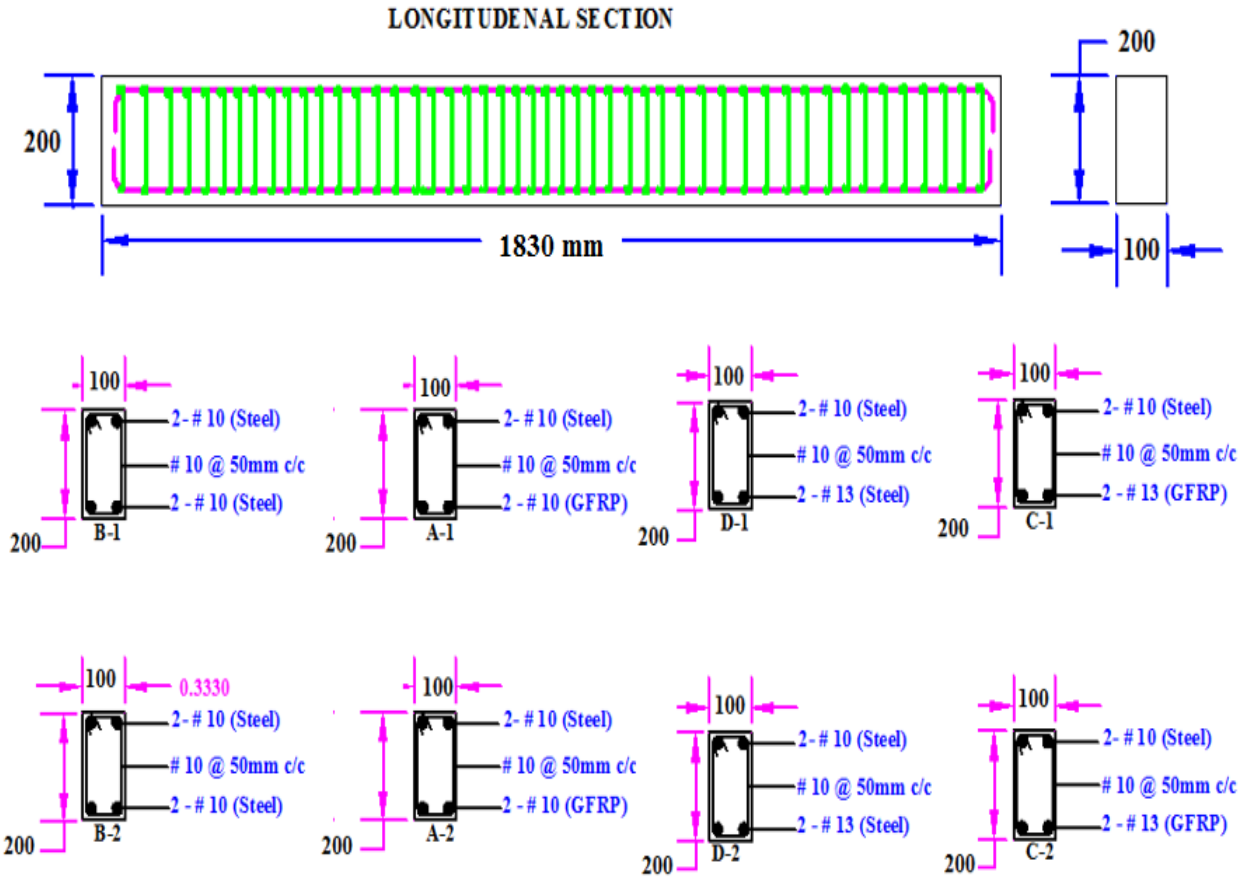

Fig. 1. Reinforcement details and test specimens

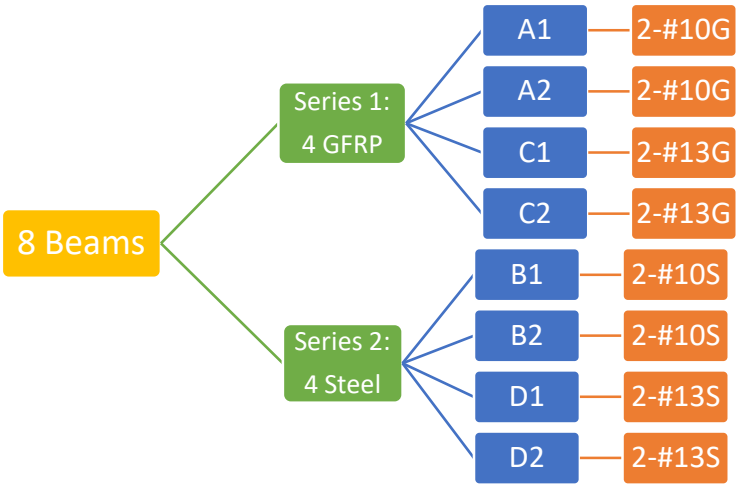

Fig. 2. Breakdown of specimens

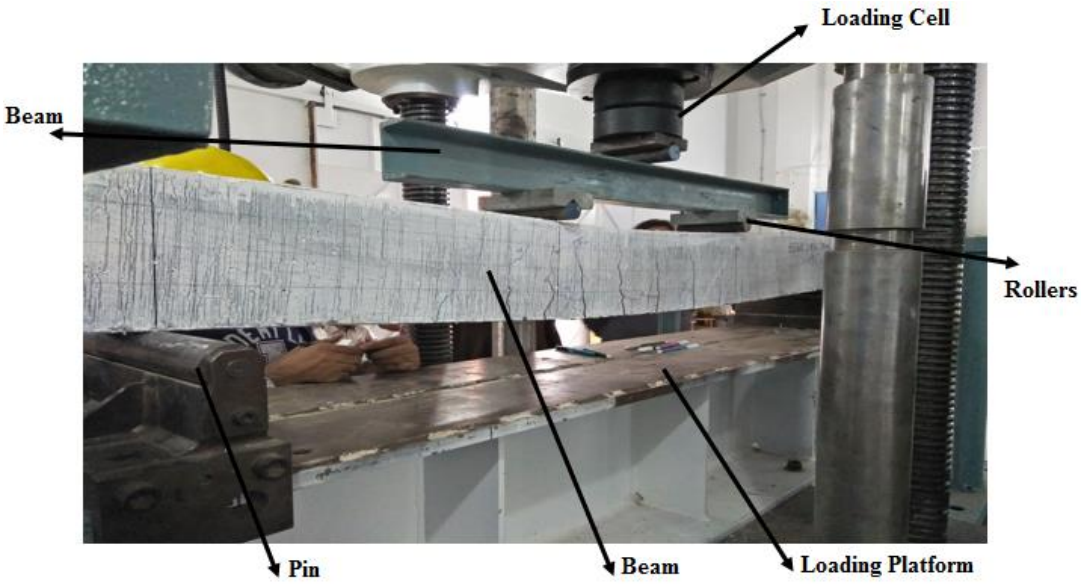

Fig. 2. Test Setup

As shown in *Fig.3*, the loading setup was a four-point loading test with a constant effective span of 1665mm measured from center to center of support. The load was applied through a pin and steel for all 8 tests. Two dial gauges were attached to the support to measure the deformation. The loading was applied at the rate of 2mm/min through 1000 kN UTM.

B. Properties of Materials

i. Mix Design for High Strength Concrete

High-strength concrete is usually defined as concrete with a 28-days compressive strength greater than 42 MPa. In this study, the following mix design was adopted with different chemicals. The maximum strength that we achieved using the following batch was 85 MPa.

Mix Design:
Ratio of Cement: Sand: Crush = 1: 1.165: 1.831
½" down crush = 70%
¾" down crush = 30%
Silica Fume, SF = 10 % of Cement
W/(C+SF) ratio=0.27
High Range Water Reducer = 1.62% of cement and silica fume
Cement: OPC
Sand: Locally available river sand
Crush: Locally available crush stone

ii. Compressive Strengths of Concrete Batches

Concrete cylindrical specimens of 150 mm diameters and 300 mm height were cast and tested for compressive strength of concrete following the ASTM C39/C39M-17a standard. The compressive strength was measured over 28 days. The average compressive strength of at least two concrete cylinders has been reported in the table. For each beam, the compressive strength was different with a maximum of 85 MPa, as shown in Table I.

TABLE I
COMPRESSIVE STRENGTHS OF CONCRETE

Beam #	Reinforcement	fc' (MPa)
A1	2-#10, GFRP	55.2
A2	2-#10, GFRP	60.6
B1	2-#10, Steel	85.2
B2	2-#10, Steel	68.8
C1	2-#13, GFRP	82.5
C2	2-#13, GFRP	84.1
D1	2-#13, Steel	61.7
D2	2-#13, Steel	84.7

iii. GFRP bar Properties

The procedure for testing the ultimate tensile strength of GFRP bars is specified in Canadian Standards Association Code (CSA S806-12).

The sample was cut from the stock of single batch bars used in the research program. Due to the nature of the sample, a test in tension following the procedure similar to the one adopted for the steel reinforcing bar is generally not possible. Applying huge pressure on GFRP bars from the end clamps results in the crushing of the bar due to low strength in the transverse direction. Therefore, the metal couplers were attached at the ends of the reinforcing bar, the type of which varied depending on the bar being tested.

A Universal testing machine was used to test the GFRP coupons in tension. The load was applied with the help of hydraulic grips. The machine was equipped with hydraulic grips. Test was performed on #13 bars and the main properties of interest are ultimate tensile strength and elongation.

Diameter of bar=12.96 mm
Area of bar=132.73 mm^2
Max. Load carried by the bar=7300 kg= 71.613 kN
Ultimate strength=Fu=540 MPa

The bar with couplers at the ends is shown in *Fig. 4.*

Fig. 3. GFRP Bar with Couplers

iv. Steel Re-Bar Properties

The steel re-bars that had been used in this testing of the beams were having a yield strength of 550 MPa and ultimate strength of 694 MPa.

III. RESULTS

In this section, the results from the four-point bending test are summarized through load-deflection curves. The presentation of results will begin with the general overview of each of the test series discussing the beam capacity and failure modes followed by in-depth presentations of the cracking patterns.

The load-deflection curves of the 8 samples are shown in *Fig. 5*.

The graphs depict that for each reinforcement ratio (ρ_f=0.84% and ρ_f=1.53%) and type of the reinforcement (GFRP or steel), overall making the four groups, A, B, C and D, the behavior of the load-deflection curve almost resembles except the initial stiffness that is higher for the beam with greater 28-days compressive strength. From each group, one beam is extracted that best represents the behavior for further study to explain the cracking pattern and ultimate loads in detail. The presentation of results will begin with a general overview of each of the test series discussing the beam capacity and failure modes followed by in-depth presentations of the cracking data.

The important parameters are highlighted on the load-deflection curves shown in *Fig. 6.* The individual observations for the specimens are summarized in the short sections to follow:

A. Specimen A2 (2- # 10, GFRP reinforced)

Cracking was first noted at 12 kN total load with a single crack developed at the right span near the point of application of four-point loading (C1 in *Fig.7*). At the mid-span, only flexural cracks developed and at the supports flexural shear cracks with no pure shear crack. The successive cracks developed at the loadings of 16 KN, 20 kN, 24 kN, 28 kN, 33 kN, 35 kN, and 54kN. The major flexural crack developed at the loading of 33 kN at an approximate distance of 350 mm from the left support and extended diagonally at the loadings of 34 and 54 kN forming the flexure shear crack, that crossed the top fibres at the point of application of loading.

The peak load observed in this specimen was 57 kN with the opening of the major crack as 3.5mm. The ultimate failure of the beam occurred because of the crushing of the concrete at the point of application of loading. The drops mainly observed in loading show the

weak bond between concrete and GFRP bars and that results in bond slippage. The failure pattern of the beam is shown in *Fig. 7.*

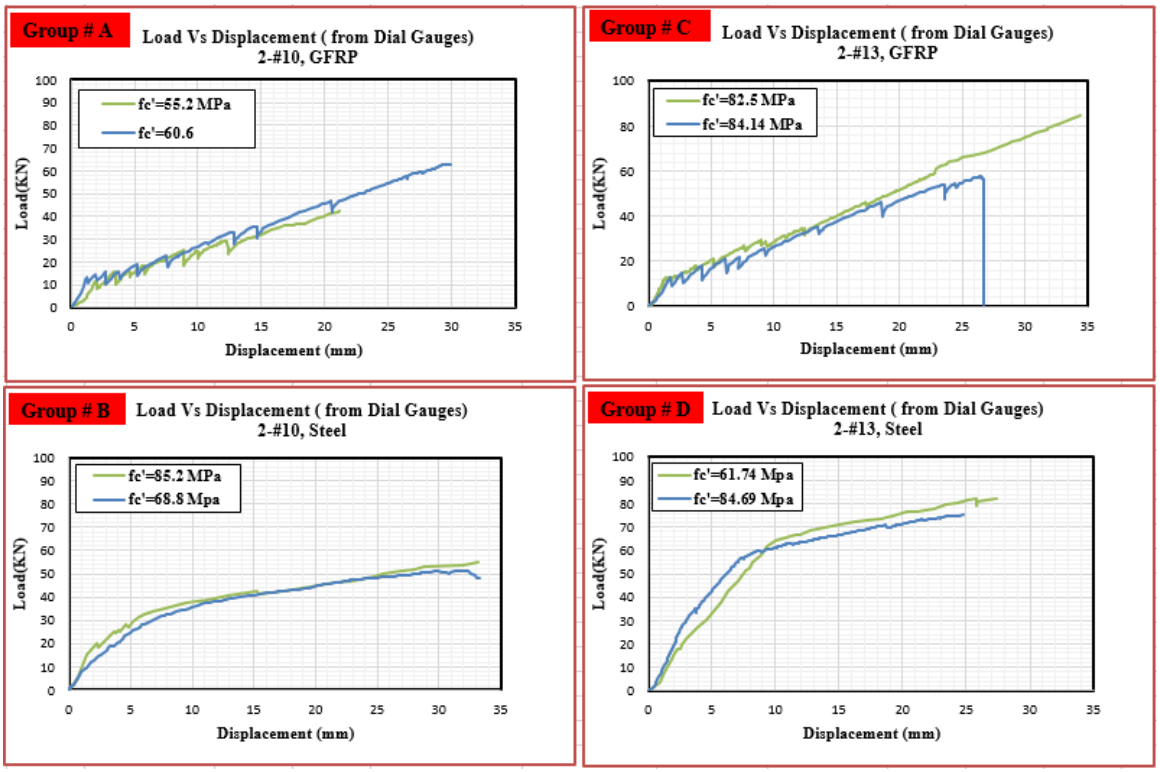

Fig. 4. Load Deflection Curves of the Beams

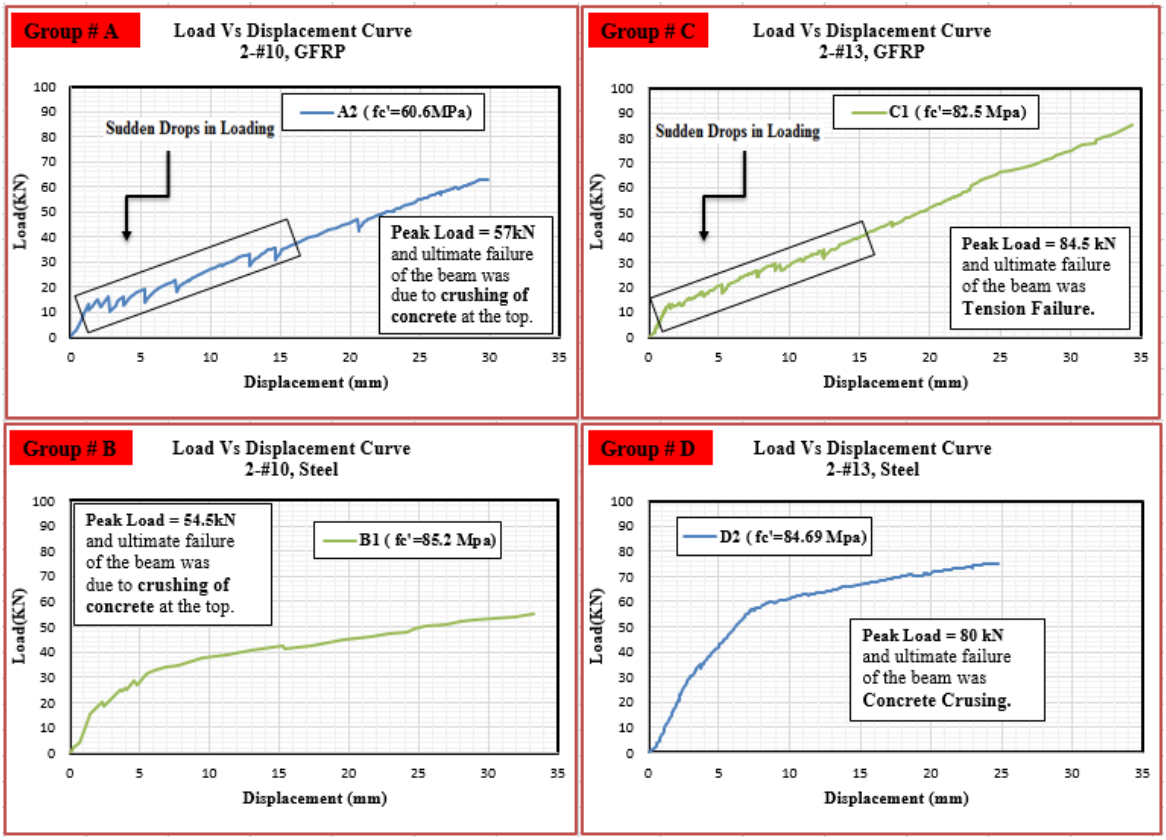

Fig. 5. Load Deflection Curves - Important Parameters

B. Specimen B1 (2- # 10, Steel Rebar reinforced)

First cracking was noted at 18 kN total load with a single crack developed nearer to the mid-span. Cracking continued with very small drops in the loading throughout the test. At the mid-span, only flexural cracks developed and at the supports flexural shear cracks with only one small pure shear crack developed near the right support. The successive cracks developed at the loadings of 28 KN, 30 kN, and 43 kN. The major flexural crack developed at the loading of 28 kN at an approximate distance of 50 mm left of the mid-span and propagated straight vertically at the loading of 40 kN and 45 kN. The crack did not cross the top fibers.

The peak load observed in this specimen was 54.5 kN with the opening of the major crack as 3.5mm. The ultimate failure of the beam was the tension failure. There were no significant drops in loadings were observed, which shows that steel has a strong bond with the concrete and there was no slippage failure. That's why the beam reinforced with steel rebars steadily took the load and a lot of warning could be observed before the final failure. The failed beam is shown in *Fig. 8*.

C. Specimen C1 (2- # 13, GFRP reinforced)

Cracking was first noted at 14 kN total load with a single crack developed at the right span near the point of application of four-point loading (C1 in *Fig.9*). At the mid-span only, flexural cracks developed and at the supports flexural shear cracks with one pure shear crack near the right support at 71 kN. The successive cracks developed at the loadings of 21 KN, 26 kN, 29 kN, 32 kN, and 35 kN. The major flexural crack developed at the loading of 29 kN at an approximate distance of 450mm from the right support and extended diagonally at the loadings of 31 and 79 kN forming the flexure shear crack, that stopped just above the neutral axis.

The peak load observed in this specimen was 84.5 kN with the maximum opening of the crack as 1.8mm. The ultimate failure of the beam occurred because of the crushing of the concrete at the mid-span top fibres. The significant drops mainly observed in loading show the weak bond between concrete and GFRP bars and that results in bond slippage. *Fig. 9* shows the failure of beam C1.

The beam C2 collapsed within no time and without any early warning because of very less ductility present in the GFRP bars. That is the main reason, despite some benefits, GFRP is not preferred in most cases keeping in view the serviceability limit states and saving the occupants' lives.

D. Specimen D2 (2- # 13, Steel Rebar reinforced)

In this test specimen, no major crack was observed. First minor cracking was noted at 35 kN total load with a single crack developed near the right support. Cracking continued with very small drops in the loading throughout the test. At the mid-span, only flexural cracks developed and at the supports flexural shear cracks with no pure shear crack. The successive cracks developed at the loadings of 54 KN, 60 kN, and 74 kN. The maximum flexural crack developed at the loading of 54 kN at an approximate distance of 50mm left of the mid-span and propagated straight vertically at the loading of 60 kN and 70 kN. The crack did not reach the top fibres.

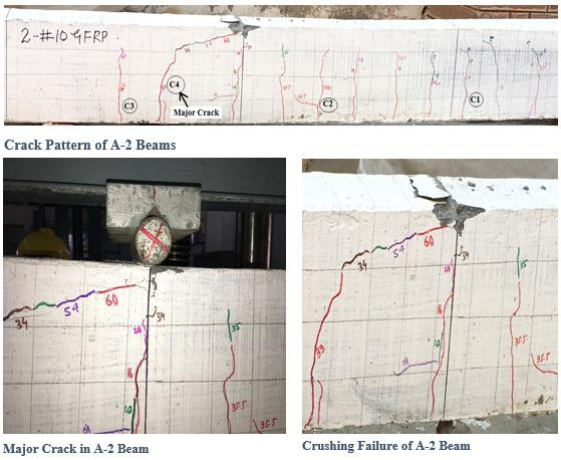

Fig.7. Failure of Beam - A2

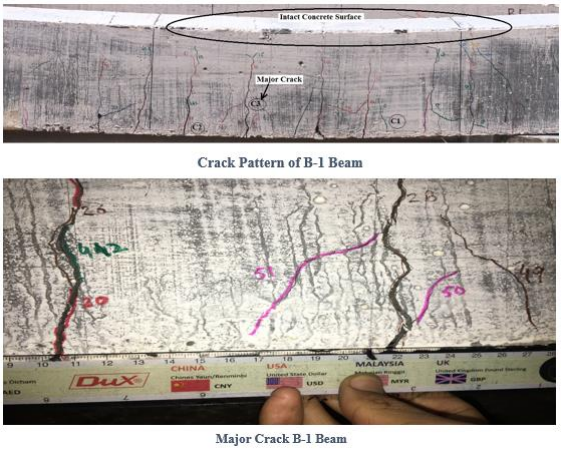

Fig.8. Failure Pattern of Beam - B1

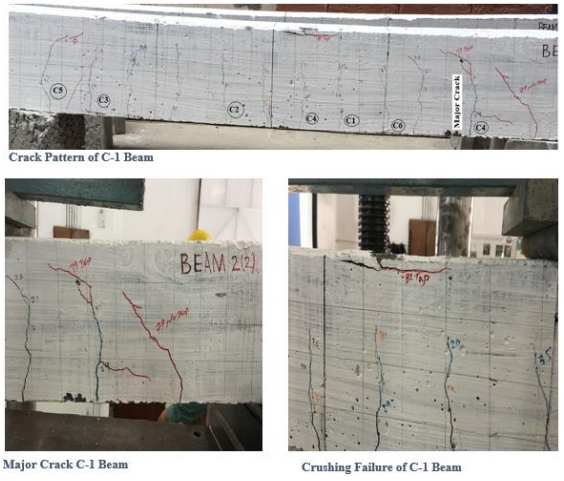

Fig. 9. Failure Pattern of Beam – C1

The peak load observed in this specimen was 80 kN with a maximum opening of the crack as 2.5mm The ultimate failure of the beam occurred because of the crushing of the concrete at the point of application of loading. There were

no significant drops in loadings, which shows that steel has a strong bond with the concrete and there was no slippage failure. *Fig. 10* shows the failure of beam D2.

Fig. 10. Failure Pattern of Beam - D2

IV. DISCUSSION

Table II summarizes the loads and deflections at the first crack and peak loads. It can be observed from the data that in the case of the GFRP RC beams (A2, C1), the reinforcement ratio had no significant effect on the first cracking loading and deflection, which were found to vary from 12kN to 14kN and 2mm to 1.5mm, respectively. However, for steel RC beams (B1, D2), there was an increase in the first cracking loading and deflection, which were found to be 18kN-35kN and 2.2-3.5mm, respectively, with the increase of reinforcement ratio from 0.835% to 1.53%. Theoretical loads listed in the table were calculated through-beam sectional analysis assuming the crushing strain of concrete as 0.003 as recommended by ACI 318-05 code [20]. Theoretical and experimental peak loads are almost the same in all the cases.

The ductility of beams is defined as their ability to sustain inelastic deformations before the failure. For steel RC beams, the ductility was calculated as the ratio of ultimate deformation to deformation at yield, which comes out to be 5.34 and 8.4 for steel RC beams (B1 and D2). With FRP reinforcement there is no yielding point, and this simple approach could not be used. Vijay and Ganga Rao [21] described that it is possible to evaluate the ductility of the FRP reinforced beams by the deformability factor (refer to Equation 1), which is defined as the ratio of the energy absorption at ultimate load to the energy absorption at the service load. From Table II, it is clear that DF increases with the increase of the reinforcement ratio.

$$Deformability\ Factor\ (DF) = \frac{Area\ under\ the\ load\ defelction\ curve\ upto\ the\ ultimate\ point}{Area\ under\ the\ load\ defelction\ curve\ upto\ the\ serviceability\ deflection, span/180} \quad Eq.1$$

TABLE II
FAILURE LOADS AND DISPLACEMENT

Specimen Code	Reinforcement	First Crack		Peak State		Theoretical Load (kN)	Serviceability Deflection(mm)	DF	Failure Mode
		P_{cr} (kN)	Δ_{cr} (mm)	P_p (kN)	Δ_p (mm)				
A2	2-#10, GFRP	12	1.3	57	30	44.95	9.25	5.84	Concrete Crushing
B1	2-#10, Steel	18	2.2	54.5	33	46.36	9.25	5.34	Tension Failure
C1	2-#13, GFRP	14	1.5	84.5	34.5	80.41	9.25	8.1	Concrete Crushing
D2	2-#13, Steel	35	3.5	80	24.5	81.94	9.25	8.4	Concrete Crushing

A. Bilinear and tri-linear Behavior

The load-deflection curve for a beam, in which the tension steel yields, can be idealized to be a tri-linear relationship as shown in the figures below. The initial slope of the curve shows the uncracked response and the stiffness of the beam. After cracking, a slight drop in the response was observed indicating the yielding stage. And finally, the third section illustrated the cracking behavior of the steel-reinforced beam. So, it is evident from the steel-reinforced concrete beams that beams kept on taking the load in these three different stages and depicted some warning even after the generation of initial cracks through the yielding of steel. However, this property is not present in the case of GFRP reinforced concrete beams, where a missing yielding zone makes the use of GFRP less favourable.

In most cases, it is sufficiently accurate to idealize the curve even further to a bilinear relationship as shown in *Fig.11* for the case of the GFRP reinforcement. As in the case of the GFRP bars, the second stage gets eliminated because of the low ductility of the beam.

The experimental results of the GFRP and steel reinforcement shown in *Fig. 11* verify the above-mentioned statements.

The following observations are made from the graphs in *Fig. 11.*

1) An elastic zone in the case of GFRP reinforced beams (A2 and C1) is very limited as compared to that of steel-reinforced beams (B1 and D2).
2) With the increase of the diameter of steel bars from 10mm to 13mm, the elastic zone increases, while in the case of GFRP the variation is insignificant.
3) The yielding zone is present in the case of steel-reinforced beams, while it is eliminated in GFRP bars.

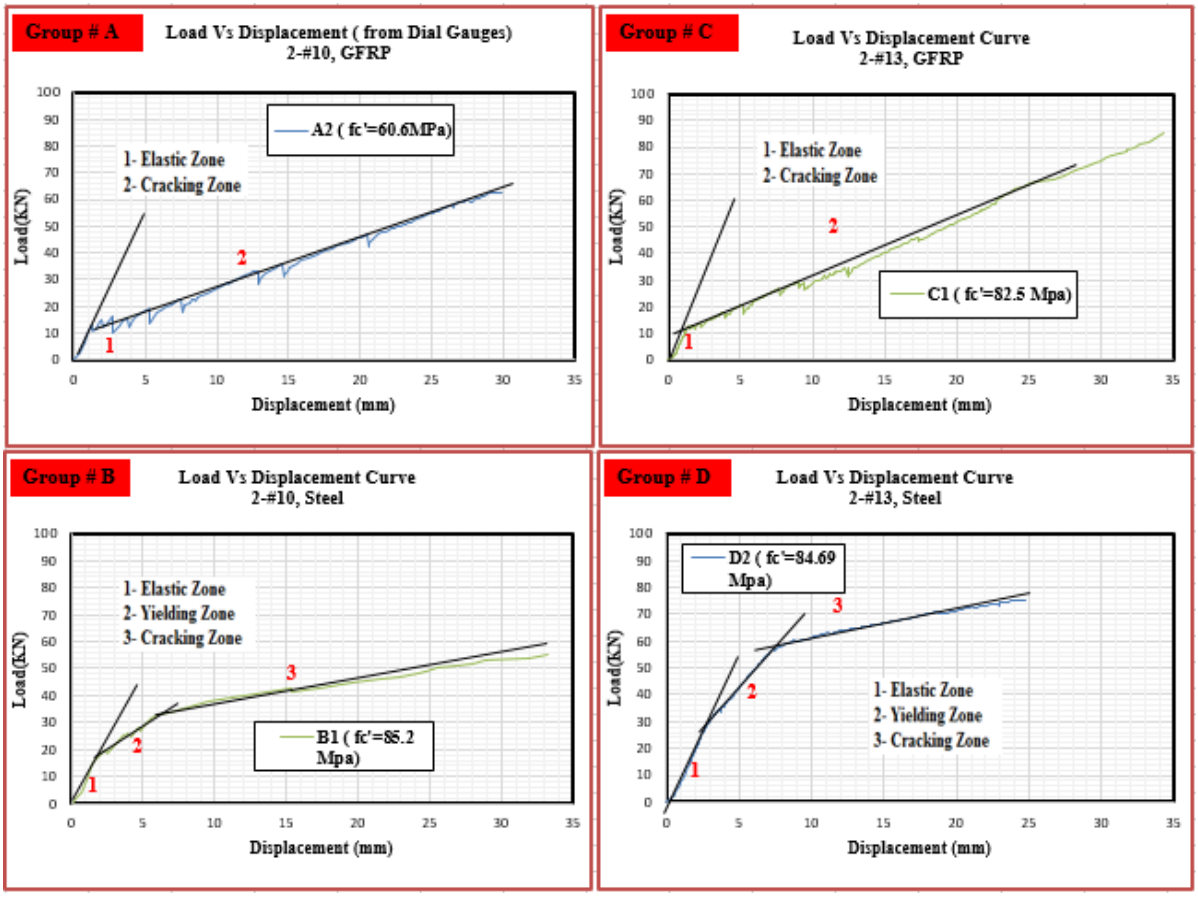

Fig. 11. Bilinear and Tri-linear Behavior of Beams

B. Behavior Prediction with Response - 2000

Reinforced Concrete Sectional Analysis software "Response 2000" [22] developed by Bentz [23] is an analytical software program. The program is employed to determine certain properties [including strength & ductility] of the structures subjected to axial, shear or moment loads. The program was used in this study to determine the capacities of the GFRP reinforced concrete beams, as well as mid-span deflection. The layered sectional analysis program Response-2000 did a good job simulating the experimental results with ratios of predicted to experimental peak loads varying from 0.90 to 0.95 and a very strong determination of the stiffness of the beam.

A comparison of experimental and predicted values is shown in *Fig. 12*. In general, Response-2000 predicted the results of GFRP reinforced concrete beams quite well as compared to steel reinforced beams considering that the program does not explicitly deal with GFRP bars. With minor modifications to the input properties of GFRP, one can obtain results from the Response-2000. Defining the same yield and ultimate strength of GFRP bars in Response – 2000 creates a mathematical bug; therefore, the ultimate strength of GFRP bars in software was defined as 0.1 MPa higher than the yield strength to avoid the error. Response-2000 was shown to be particularly strong in estimating the stiffness of the beam, failure deflection and failure loads in the case of steel reinforcement as well as GFRP reinforcement.

Custom input was provided to define the stress-strain behavior of the GFRP reinforcement bars. Overall, the software predicted the failure loads, displacements and stiffness of both steel and GFRP reinforced beams with more than 90% accuracy.

V. CONCLUSION

Results of an investigation into understanding the flexural behavior of concrete beams reinforced with the GFRP bars have been presented in this paper. Observations have led to the following conclusions:

1) The load-deflection behavior of the high strength concrete beams reinforced with GFRP bars displayed a bi-linear response, however, the load-deflection behavior of the high strength concrete beams reinforced with ordinary steel bars displayed a tri-linear response

2) Load carrying capacity was found to be increased as concrete strength and reinforcement ratio increased regardless of reinforcement type. Similarly, the initial beam stiffness showed to be increased as concrete strength increased in both types of reinforcements; GFRP and steel.

3) Significant drops in loading were observed in GFRP RC beams which show the weak bond between the concrete and GFRP bar, while drops in loading were not significant in the case of steel reinforcement.

4) Layered sectional analysis program Response-2000 also did a good job simulating the experimental results with ratios of predicted to experimental peak loads varying from 0.90 to 0.95 and a very strong determination of stiffness of the beam.

VI. RECOMMENDATIONS

The present study compared the bending behavior of steel and GFRP reinforced concrete beams.

However, further research is warranted in the following areas:

1) The effects of different types of fibers (Aramid and Carbon) should be investigated by constructing and testing the beams as designed in the current study.

2) Bond behavior of GFRP bars to concrete should be further investigated, and recommendations need to be made to improve the bond performance.

Fig. 12.

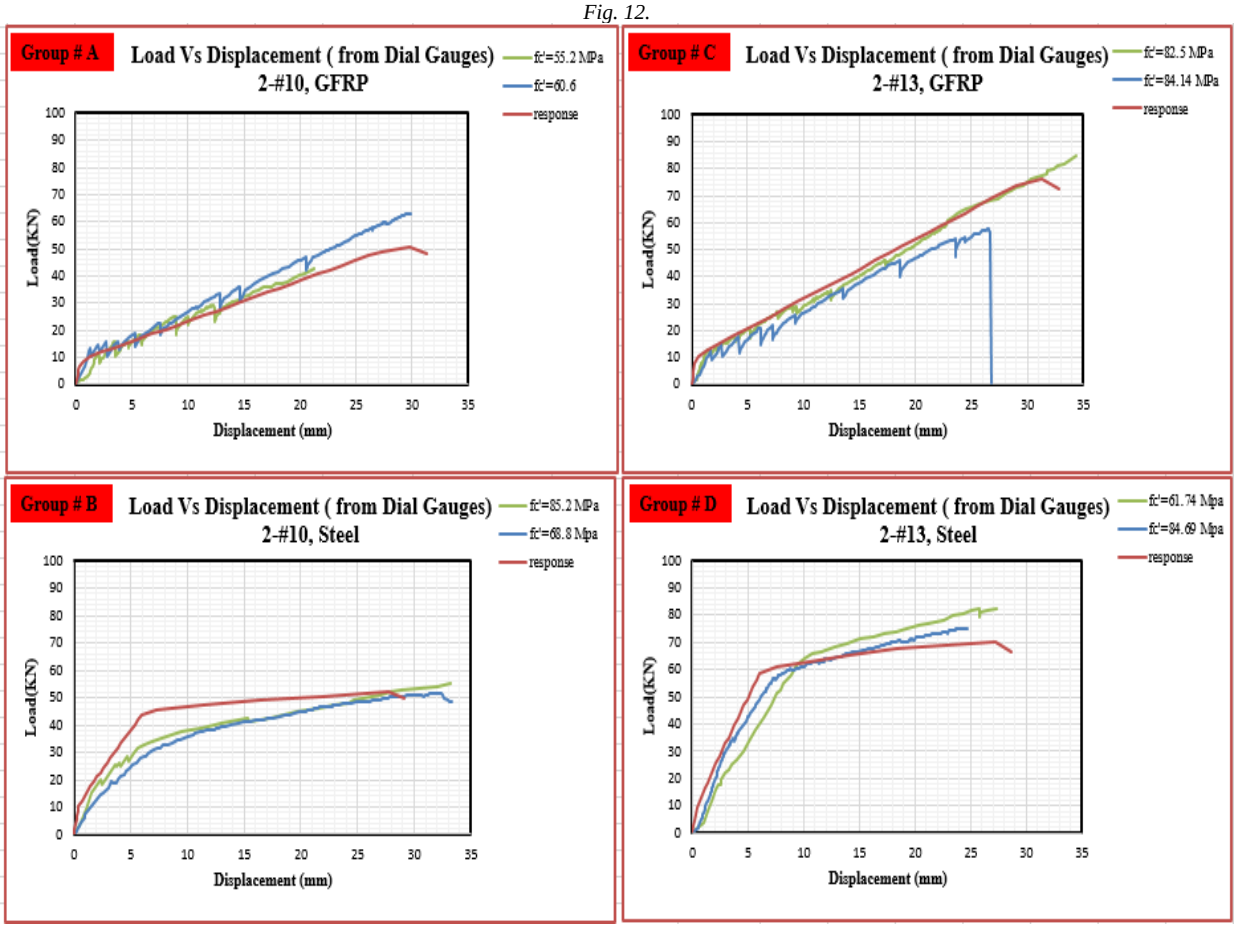

Response 2000 Predictions

REFERENCES

[1] Committee, A. Guide for the design and construction of structural concrete reinforced with FRP bars. Vol. ACI 440.1 R 2006:6.

[2] Saadatmanesh H, Ehsani MR. Application of fibre-composites in civil engineering. In: Structural materials. ASCE; 1989.

[3] Ballinger CA. Development of composites for civil engineering. In: Advanced Composites Materials in Civil Engineering Structures. ASCE; 1991.

[4] Nanni A, Al-Zaharani M, Al-Dulaijan S, Bakis C, Boothby 1. 17 bond of FRP reinforcement to concrete experimental results. In: Non-metallic (FRP) Reinforcement for Concrete Structures: Proceedings of the Second International RILEM Symposium. CRC Press; 1995.

[5] Federation International du Beton, FIB, Task Group 9.3. FRP reinforcement in RC structures, Lausanne, Switzerland; 2007.

[6] Attari N, Amziane S, Chemrouk M. Flexural strengthening of concrete beams using CFRP, GFRP and hybrid FRP sheets. Constr Build Mater;Vol. 37(0), pp. 746-57. 2012.

[7] Smith ST, Hu S, Kim SJ, Seracino R. FRP-strengthened RC slabs anchored with FRP anchors. Eng Struct;33(4):1075-87. 2011.

[8] Li G, Kidane S, Su-Seng P, Helms JE, Stubblefield MA. Investigation into FRP repaired RC columns. Compos Struct;Vol. 62(1),pp. 83-9. 2003.

[9] Alsayed SH. Flexural behavior of concrete beams reinforced with the GFRP bars. Cement Concr Compos; Vol. 20(1):pp. 1-11. 1997.

[10] Noel M, Soudki K. Estimation of the crack width and deformation of FRP-reinforced concrete flexural members with and without transverse shear reinforcement. Eng Struct;Vol. 59,pp. 393-8. 2014.

[11] Kalpana VG, Subramanian K. Behavior of concrete beams reinoforced with GFRP bars. J Reinf Plast Compos;Vol. 30(23):pp. 1915-22. 2011.

[12] Ashour AF, Habeeb MN. Continuous concrete beams reinforced with CFRP bars. Proceedings of the institution of civil engineers: structures and buildings;Vol. 161(6):pp. 349-57. 2008.

[13] Saadatmanesh H. Fibre composites for new and existing structures. ACI Mater J;Vol. 91(3), pp.346-54. 1994.

[14] Tighiouart B, Benmokrane B, Gao D. Investigation of bond in concrete member with the fibre reinforced polymer (FRP) bars. Contruct Build Mater;Vol. 12(8),pp. 453-62. 1998.

[15] Benmokrane B, Tighiouart B, Chaallal O. Bond strength and load distribution of composite GFRP rebars in concrete. ACI Mater J;Vol. 93(3),pp. 246-53. 1996.
[16] Chaallal O, Benmokrane B. Pullout and bond of glass fibre rods embedded in concrete and cement grout. Mater Struct;Vol. 26(3),pp. 165-75. 1993.
[17] Toutanji HA, Saafi M. Flexural behavior of concrete beams reinforced with glass fibre-reinforced polymer (GFRP) bars. ACI Strcut J 2000;Vol. 97(5),pp. 712-9.
[18] ACI Committee 440. Guide for the design and construction of structural concrete reinforced with FRP bars. Farmington Hill (MI): ACI;2006.
[19] Benmokrane B, Zhang B, Chennouf A. Tensile properties and pullout behavior of AFRP and CFRP rods for grouted anchor applications. Constr Build Mater;Vol. 14(3):pp. 157-70. 2000.
[20] ACI Committee 318. Building code requirements for structure concrete and commentary (ACI 318-05/ACI 381R-05). Detroit, Michigan (USA): American Concrete Institute; 2005.
[21] Vijay P, Ganga Rao V. Bending behavior and deformability of the glass fibre-reinforced polymer concrete members. ACI Struct J;Vol. 98(6),pp. 834-42. 2001.
[22] Bentz, E.C. (2000) "Sectional Analysis of Reinforced Concrete", PhD Thesis, Department of Civil Engineering, University of Toronto, 2000.
[23] Bentz, E.C. (2000), "Response 2000 Bugs", http://www.ecf.utoronto.ca/~bentz/r2k.htm, 2000.